Electronic Supplementary Material (ESI) for Journal of Materials Chemistry A.

Supporting Information

Synthesis, characterization and photovoltaic properties of electron accepting azadipyrromethene-based dyes: effect of pyrrolic substituents

Wasana Senevirathna, Jia-yu Liao, Zhenghao Mao, Jun Gu, Matthew Porter, Chunlai Wang,

*Roshan Fernando, Geneviève Sauvé**

Department of Chemistry, Case Western Reserve University, Cleveland, Ohio 44106, USA

Table of Contents

Synthesis of A4 and A5 ....S2
NMR spectra S6
MALDI-TOF-MS spectra S12
TGA graphs and data S13
Cyclic voltammetry graphs S14
Optical properties..S16
P3HT Fluorescence quenching graphs..S19
AFM and Solar cells S20
References..S24

Synthesis of A4 and A5

tributyl(4-(2-ethylhexyloxy)phenylethynyl)tin (A4)

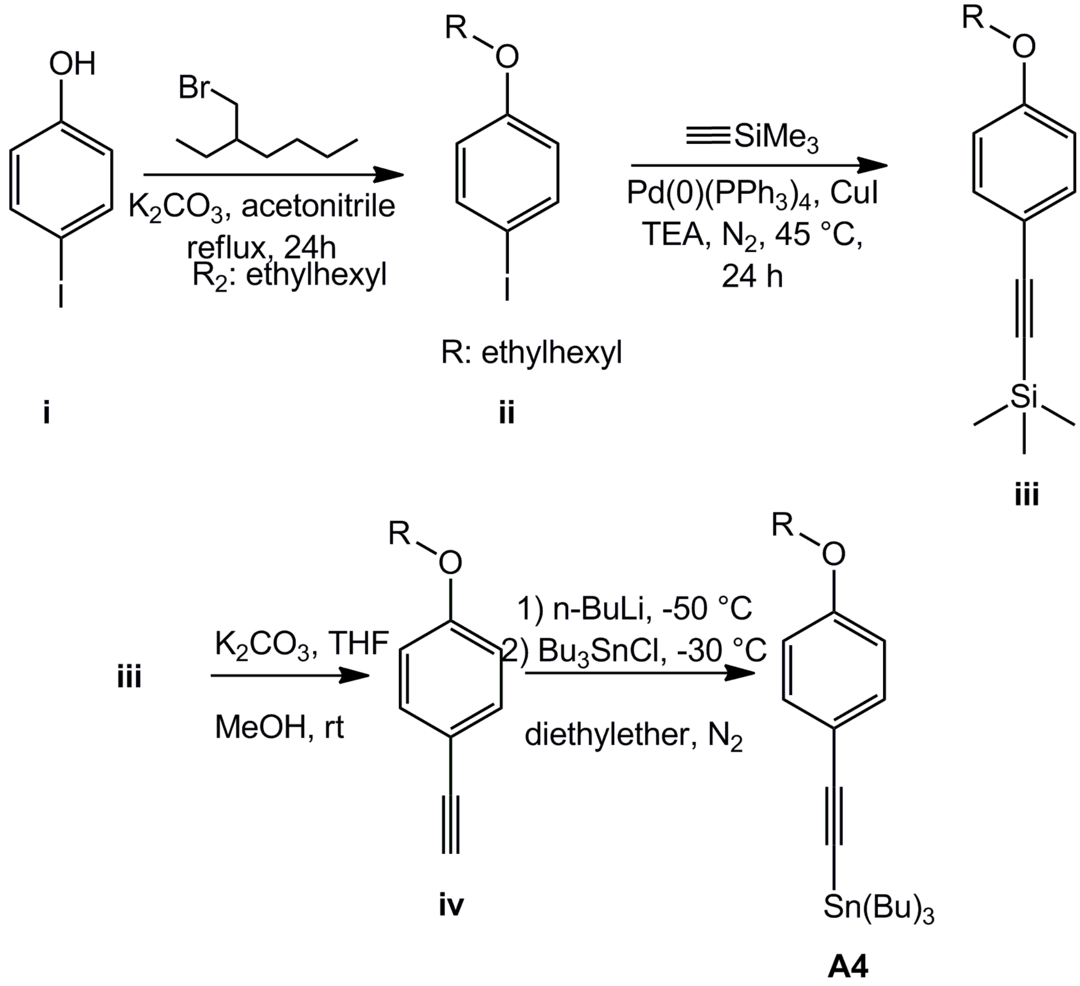

Scheme S1. Synthesis route of tributyl(4-(2-ethylhexyloxy)phenylethynyl)tin (**A4**).

In a 500 mL flask, 4-iodophenol (**i**) (10 g, 0.045 mol), 2-ethylhexylbromide (27 g, 0.140 mol), K_2CO_3 (20 g, 0.140 mol) were dissolved in acetonitrile (175 ml). The mixture was refluxed for 36-48 h. During the course of the reaction, potassium carbonate did not completely dissolve. After cooling down to room temperature, the solid was removed by gravity filtration, and the solvent was removed by rotary evaporation. The pale yellow oil was extracted with ether and washed with water. The ether layer was dried over anhydrous $MgSO_4$. The solvent was removed by vacuum evaporation. Thin layer chromatography (TLC) with hexane showed only one spot indicating the presence of the product. The excess of ethylhexyl bromide was removed by distillation and a plug was carried out using silica gel and hexanes. A pale yellow oil was obtained (**ii**). Yield 13.62 g, 91%. ^{1}H NMR (400 MHz, $CDCl_3$, δ): 7.51-7.55 (dd, 2H), 6.66-6.69 (dd, 2H), 3.78-3.80(dd, 2H), 1.68-1.74 (m, 1H), 1.38-1.45 (m, 4H), 1.29-1.32 (m, 4H), 0.86-0.92 (m, 6H).

In a 500 mL flask, 2-ethylhexyloxy-4-iodobenzene (**ii**) (13.62 g, 0.041 mol) was dissolved in triethylamine (150 mL). CuI (400 mg, 4 %), $Pd(PPh_3)_4$ (1.0 g, 2 %) and trimethylsilylacetylene (6.0 g, 0.062 mol) were added and stirred under N_2 at 45 °C for 24 h. The solid was removed by gravity filtration and washed with ether. A plug was carried out using silica gel/toluene. The yellow oily residue (**iii**) was obtained and was used as it is in the next step. ^{1}H NMR (400 MHz, $CDCl_3$, δ): 7.37-7.40 (dd, 2H), 6.78-6.82 (dd, 2H), 3.80-3.82(dd, 2H), 1.68-1.72 (m, 1H), 1.36-1.53 (m, 4H), 1.27-1.31 (m, 4H), 0.86-0.90 (m, 6H), 0.19-0.25 (m, 9H).

In a 250 mL flask, ((4-((2-ethylhexyl)oxy)phenyl)ethynyl)trimethylsilane (**iii**) (assuming 0.045 mol) was dissolved in mixture of 2:1 THF-MeOH (300 mL). In a separate container, potassium carbonate (28 g, 5 eq) was dissolved in 100 mL of methanol. Both mixtures were combined and stirred at room temperature for 12 h. The solution was filtered through Celite and extracted with ether. The organic layer was washed with water (100 mL ×3) and dried over anhydrous $NaSO_4$. The solvent was removed by rotary evaporation. The crude product was purified by column chromatography with silica gel and hexanes, and then with DCM: hexanes ramping from 0 to 20 %. The first fraction was collected and the solvent was removed by rotary evaporation. A yellow oil was obtained (**iv**). Yield 5.72 g. ^{1}H NMR (400 MHz, $CDCl_3$, δ): 7.38-

7.42 (dd, 2H), 6.80-6.84 (dd, 2H), 3.82-3.83(dd, 2H), 2.98 (s, 1H), 1.68-1.74 (m, 1H), 1.35-1.44 (m, 4H), 1.25-1.30 (m, 4H), 0.86-0.90 (m, 6H).

In a 250 mL flask, 1-(2-ethylhexyloxy)-4-ethynylbenzene (**iv**) (4.2 g, 18.26 mmol) was charged. The flask was vacuumed and refilled (×3) with N_2. Then 20 mL of dry diethyl ether was added and degassed with nitrogen for 5 min. The flask was cooled to -61°C using a $CHCl_3$/dry ice bath. n-BuLi (2.5 M in hexanes 8 mL, 18.26 mmol) was added via a syringed dropwise. After ~10-15 min the cold bath was removed and the reaction mixture was allowed to reach room temperature. The solution turned pale brown. After 30 min, the reaction mixture was cooled to -42 °C using an acetonitrile/dry ice bath. Bu_3SnCl (5 mL, 19 mmol) was added via a syringe dropwise. After ~ 10 min, the cold bath was removed and the reaction mixture was allowed to reach room temperature. Upon warming, a white suspension was formed. After stirring at room temperature for ~1 h, the mixture was dried by rotary evaporation. The oily residue was dissolved in hexanes (or pentanes) and vacuum filtered. The filtrate was taken and the solvent was removed by rotary evaporation. A heavy yellow oil was obtained (**A4**). Yield: 10.0 g, ~99%. ^{1}H NMR (400 MHz, $CDCl_3$, δ): 7.35-7.37 (dd, 2H), 6.77-6.79 (dd, 2H), 3.80-3.81(dd, 2H), 1.68-1.74 (m, 1H), 1.32-1.44 (m, 10H), 1.26-1.31 (m, 4H), 1.56-1.64 (m, 6H), 1.01-1.05 (m, 6H), 0.86-0.96 (m, 15H).

tributyl((5-(2-ethylhexyl)thiophen-2-yl)ethynyl)tin (A5)

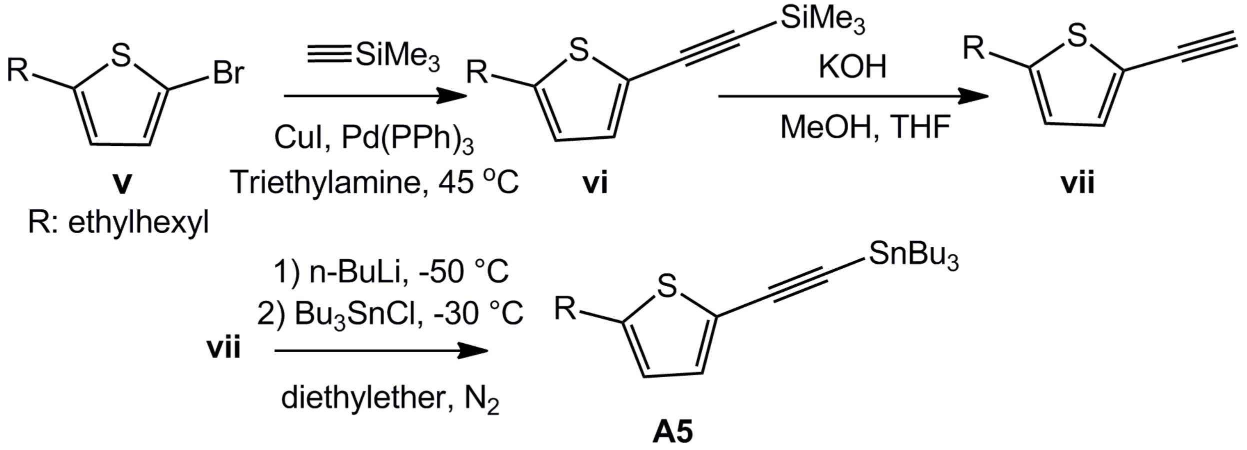

Scheme S2. Synthesis route of tributyl((5-(2-ethylhexyl)thiophen-2-yl)ethynyl)tin **(A5)**.

2-bromo-5-(2-ethylhexyl)thiophene (**v**) was synthesized according to a literature procedure.[S1] 2-bromo-5-(2-ethylhexyl)thiophene (6.0 g, 21.8 mmol) and trimethylsilylacetylene (3.20 g, 32.7 mmol) were dissolved in 100 mL triethylamine and degassed for 15 min. $Pd(PPh_3)_2Cl_2$ (1.5 g) and CuI (414 mg) were added. The reaction mixture was stirred at 60 °C under N_2 for 24 h. The solvent was removed by rotary evaporation. The crude was purified by column chromatography with silica gel and hexanes. A pale yellow oil was obtained (**vi**). Yield: 5.1 g, 17.5 mmol, 80%.

Potassium hydroxide (4 eq) was dissolved in 2:1 THF/MeOH (300 mL). The solvent mixture was transferred into ((5-(2-ethylhexyl)thiophen-2-yl)ethynyl)trimethylsilane (**vi**). The reaction mixture was stirred at room temperature for overnight. The product was extracted with hexanes and washed with water (100 mL ×3). The organic layer was dried over anhydrous $MgSO_4$. The crude was purified by column chromatography with silica gel and hexanes. An orange color oil was obtained (**vii**). Yield: 3.8 g 96 %. ^{1}H NMR (400 MHz, $CDCl_3$, δ): 7.05-7.09

(d, 2H), 6.59-6.60 (d, 1H), 3.22 (s, 1H), 2.64-2.65 (d, 2H), 1.7 (m, 1H), 1.26-1.31 (m, 8H), 0.80-0.88 (m, 9H).

The final product **A5** was synthesized using the same procedure as that for **A1**, using 2-(2-ethylhexyl)-5-ethynylthiophene (**vii**). A yellow oil was obtained **(A5)**. Yield: 8.4 g 97%. ^{1}H NMR (400 MHz, CDCl$_3$, δ): 6.98-6.99 (d, 1H), 6.55-6.56 (d, 1H), 2.67-2.68 (d, 2H), 1.54-1.57 (m, 1H), 1.30-1.37 (m, 26H), 0.85-0.92 (m, 15H).

^{1}H and ^{19}F NMR Spectra

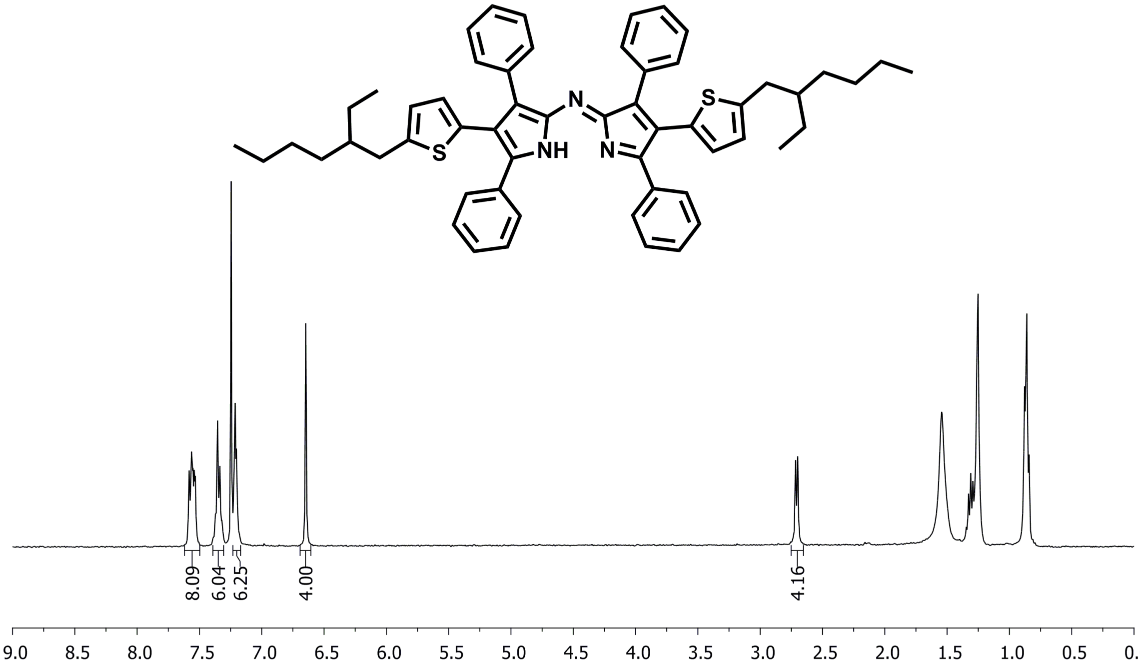

Figure S1. 400 MHz ^{1}H NMR of H(WS2).

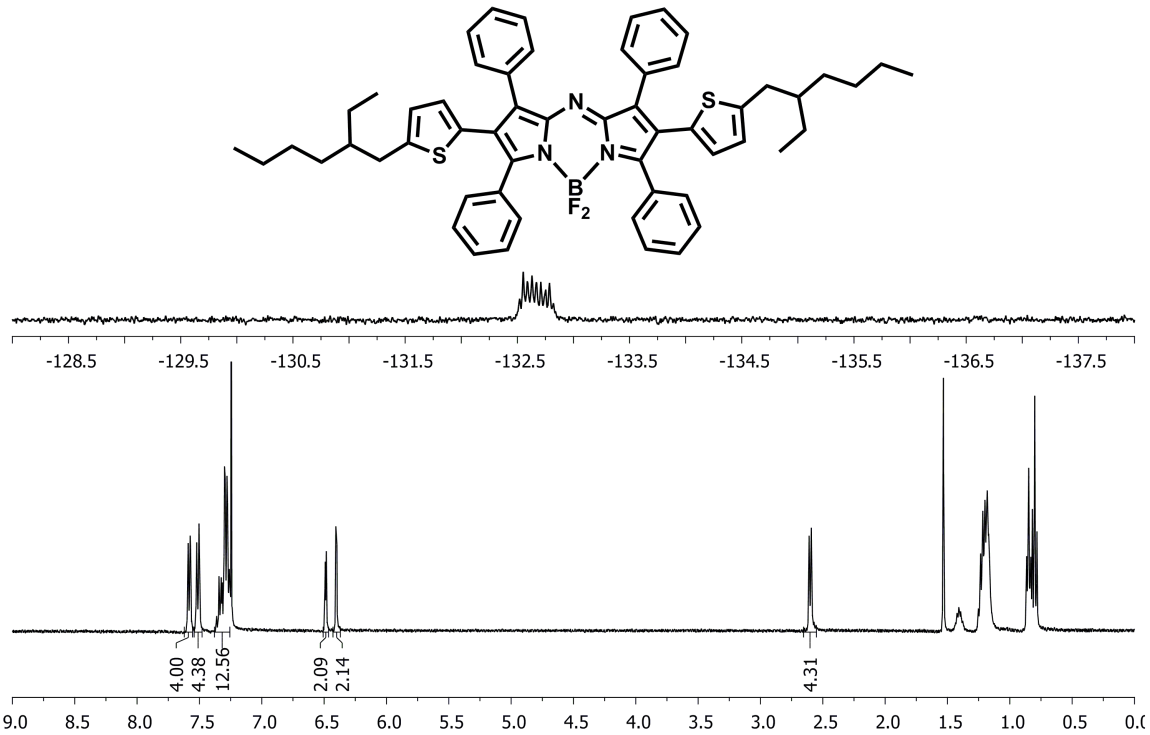

Figure S2. 400 MHz ^{1}H NMR (bottom) and ^{19}F NMR (top) of BF_2(WS2).

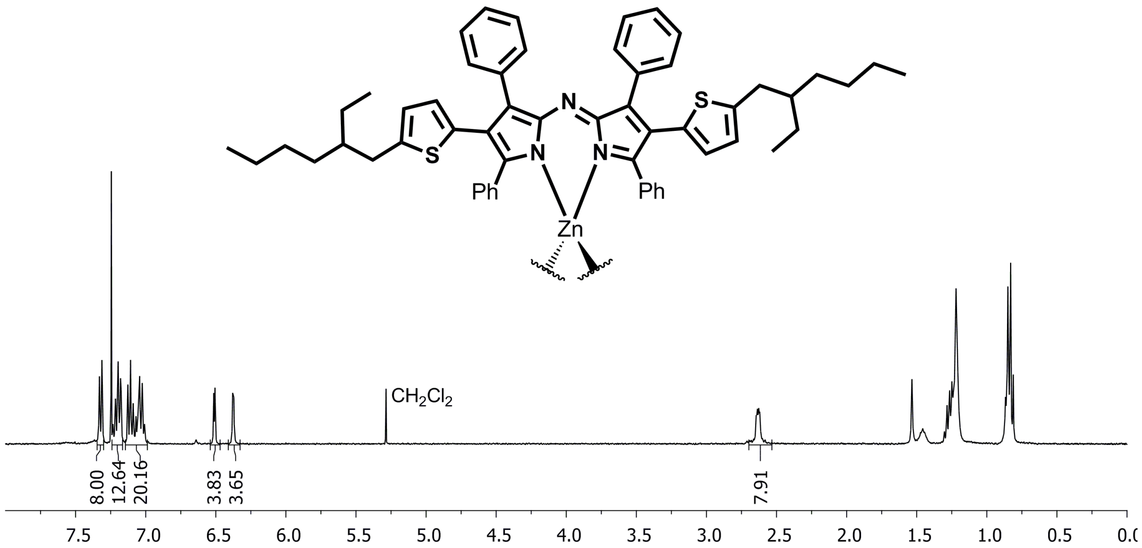

Figure S3. 400 MHz ^{1}H NMR of Zn(WS2)$_2$.

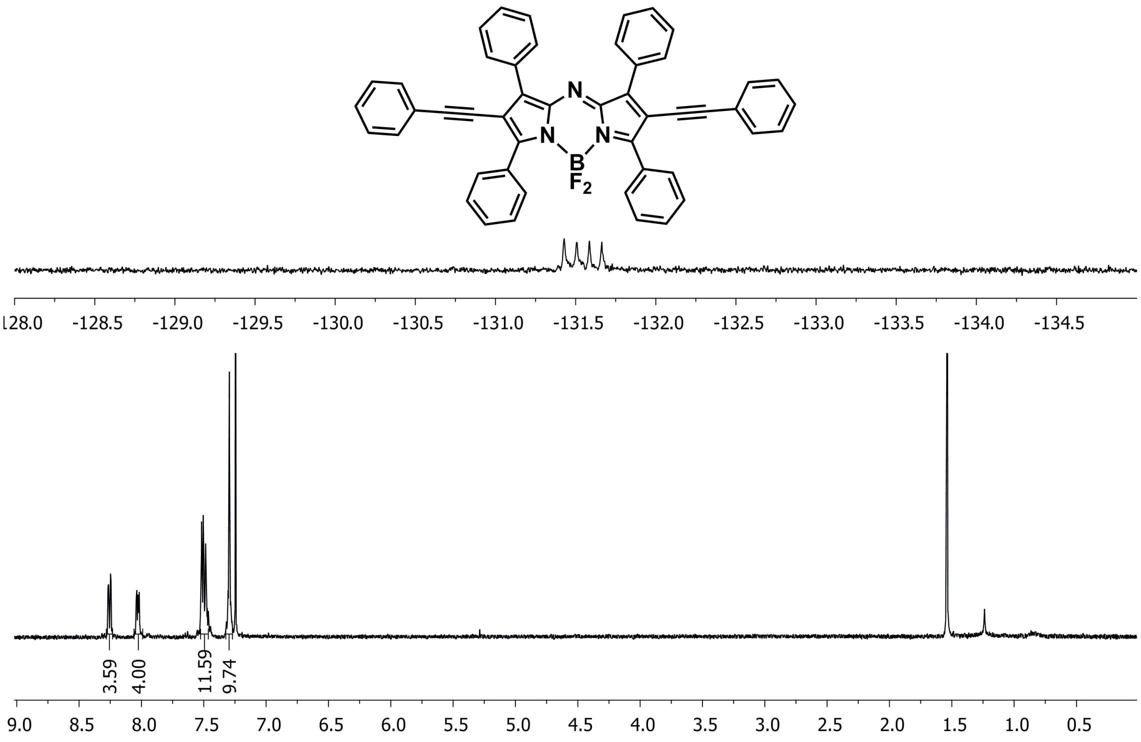

Figure S4. 400 MHz ^{1}H NMR (bottom) and ^{19}F NMR (top) of BF$_2$(WS3).

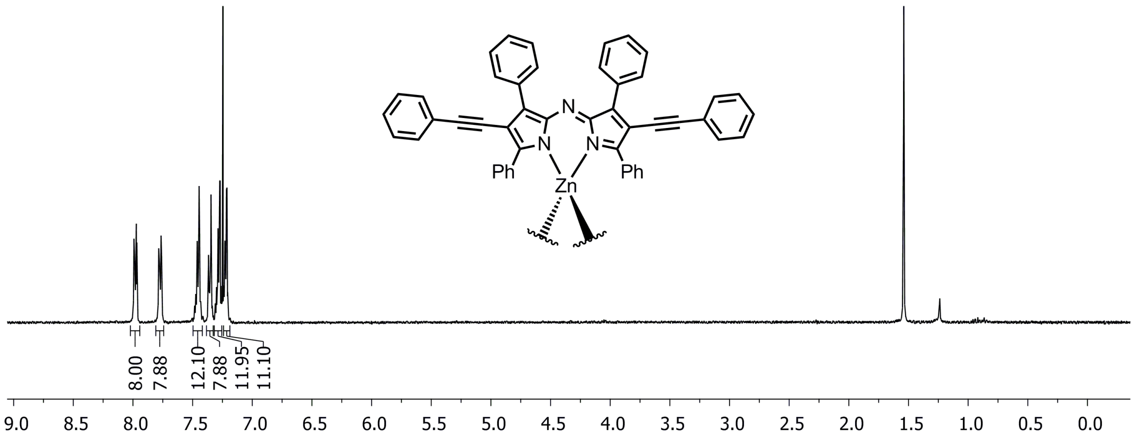

Figure S5. 400 MHz ^{1}H NMR of Zn(WS3)$_2$.

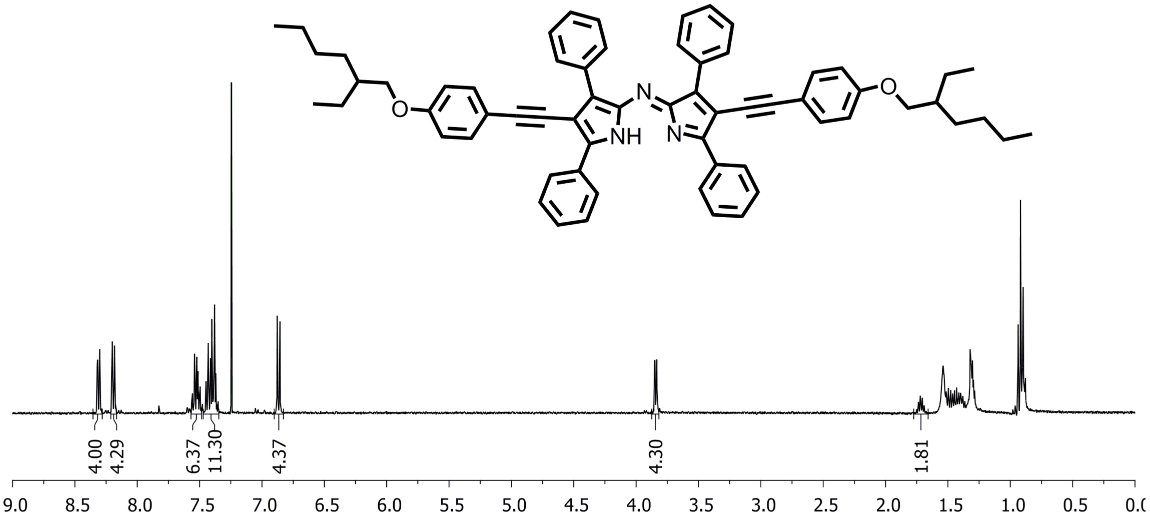

Figure S6. 400 MHz ^{1}H NMR of H(WS4).

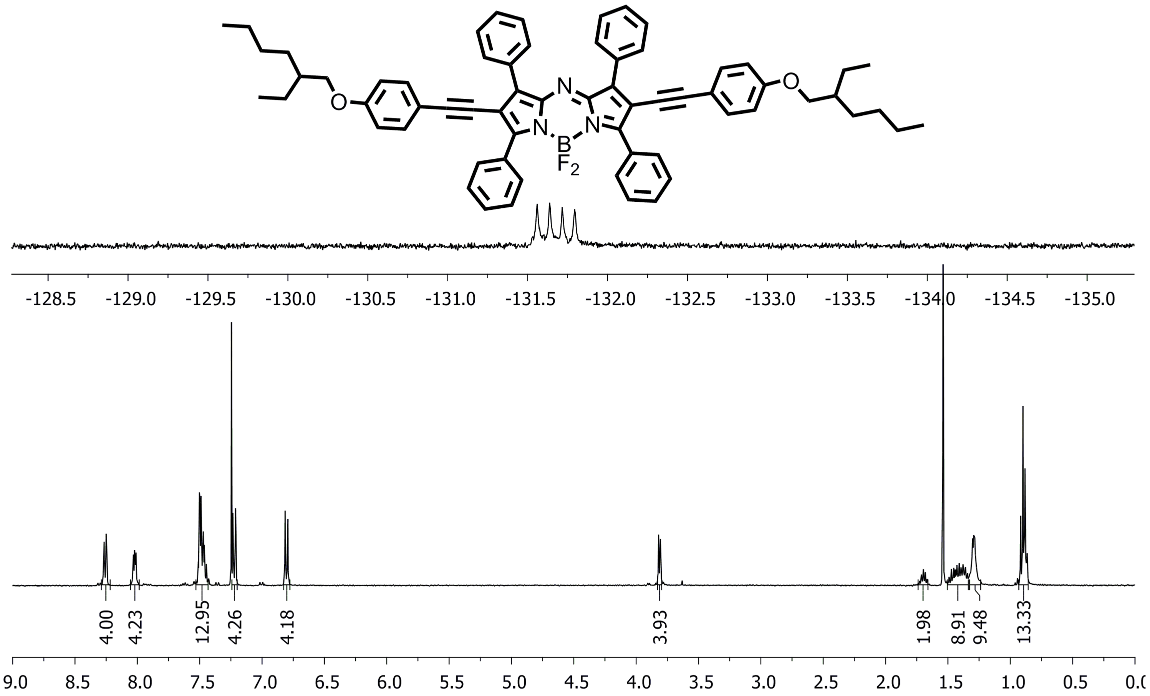

Figure S7. 400 MHz ^{1}H NMR (bottom) and ^{19}F NMR (top) of BF_2(WS4).

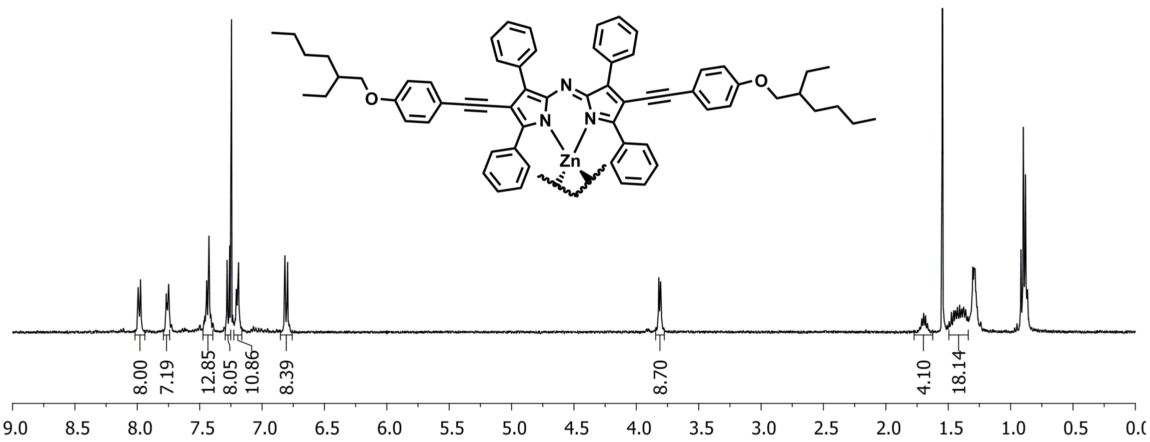

Figure S8. 400 MHz ^{1}H NMR of Zn(WS4)$_2$.

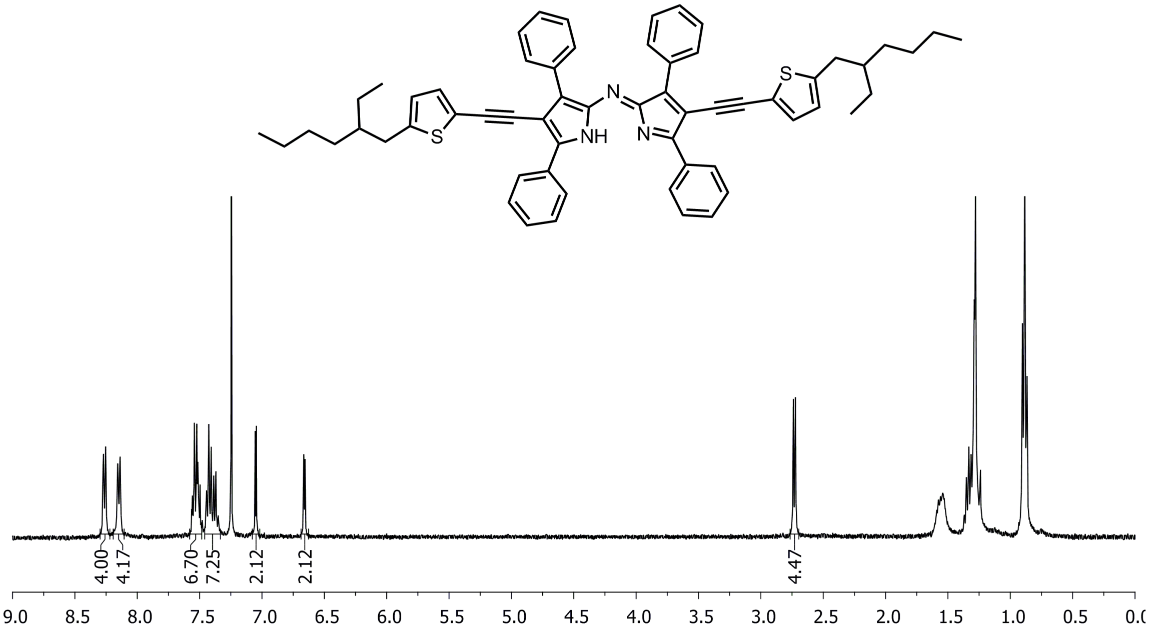

Figure S9. 400 MHz ^{1}H NMR of H(WS5).

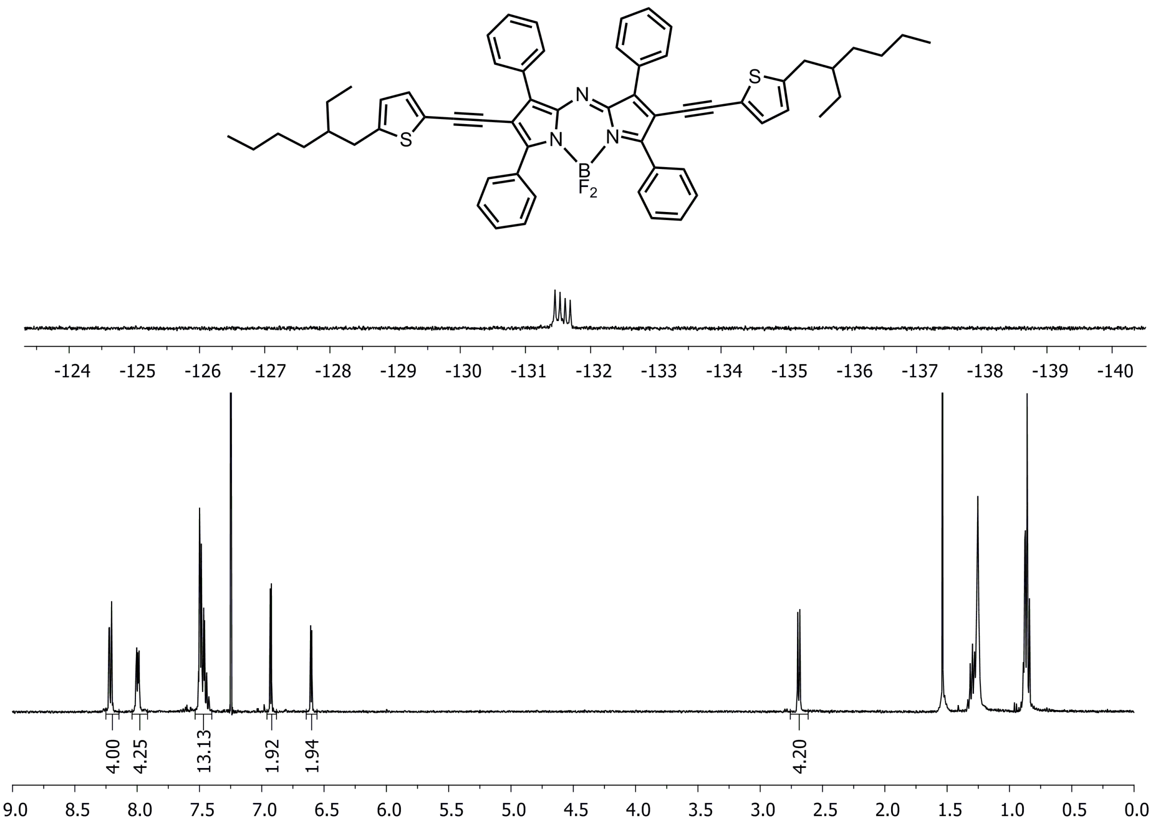

Figure S10. 400 MHz ^{1}H NMR (bottom) and ^{19}F NMR (top) of BF$_2$(WS5).

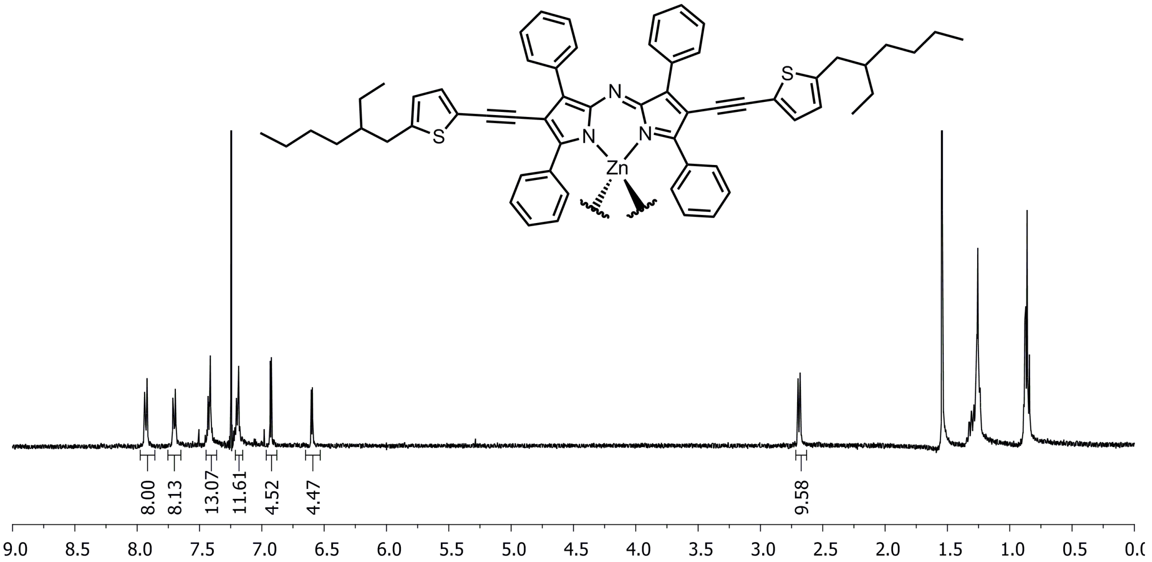

Figure S11. 400 MHz ^{1}H NMR of Zn(WS5)$_2$.

MALDI-TOF MS Spectra

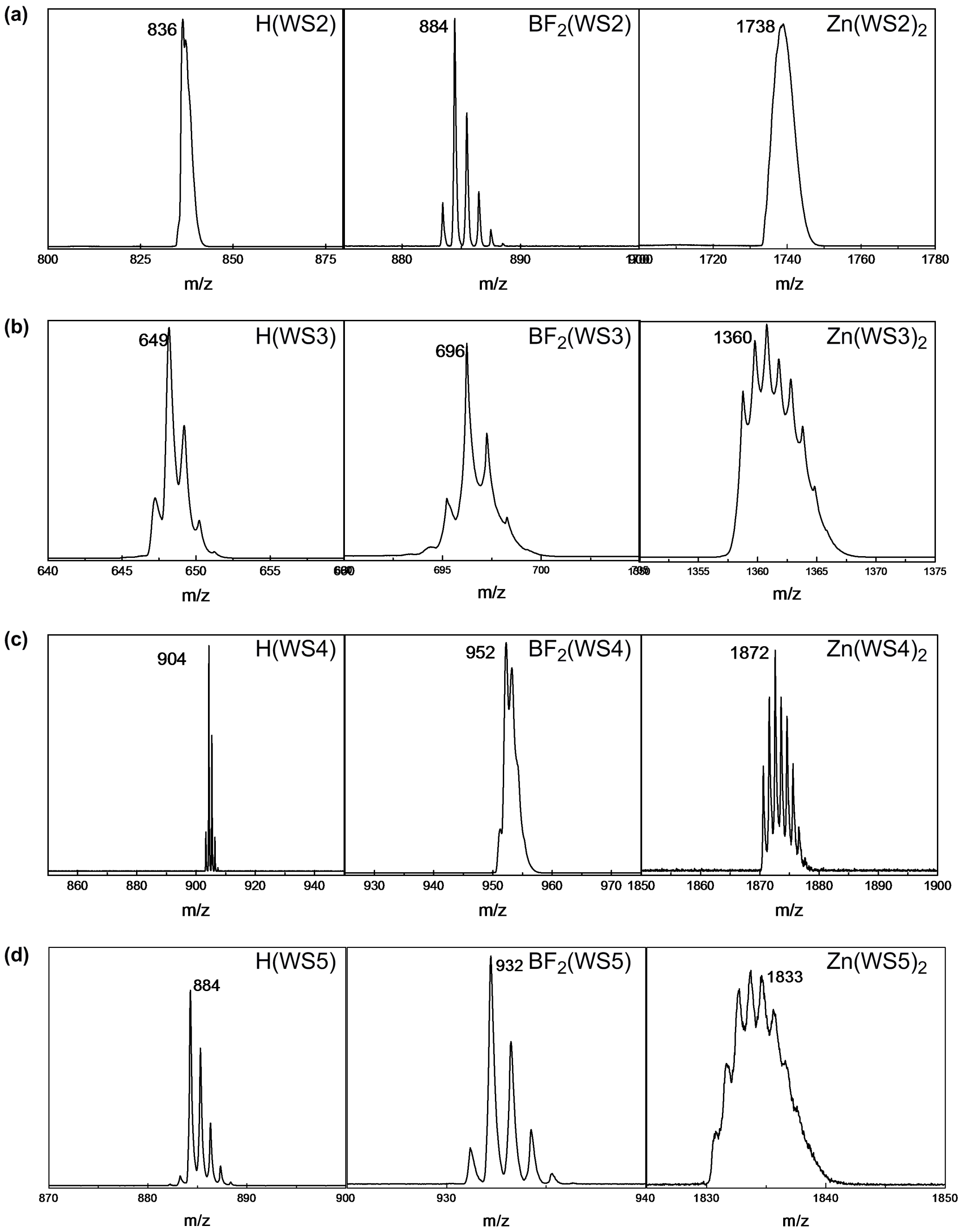

Figure S12. MALDI-TOF Mass Spectrum of (a) H(WS2), BF_2(WS2), and Zn$(WS2)_2$, (b) H(WS3), BF_2(WS3), and Zn$(WS3)_2$, (c) H(WS4), BF_2(WS4), and Zn$(WS4)_2$, and (d) H(WS5), BF_2(WS5), and Zn$(WS5)_2$ (Isotope pattern of the molecular ion in reflective negative mode).

Thermal Gravimetric Data

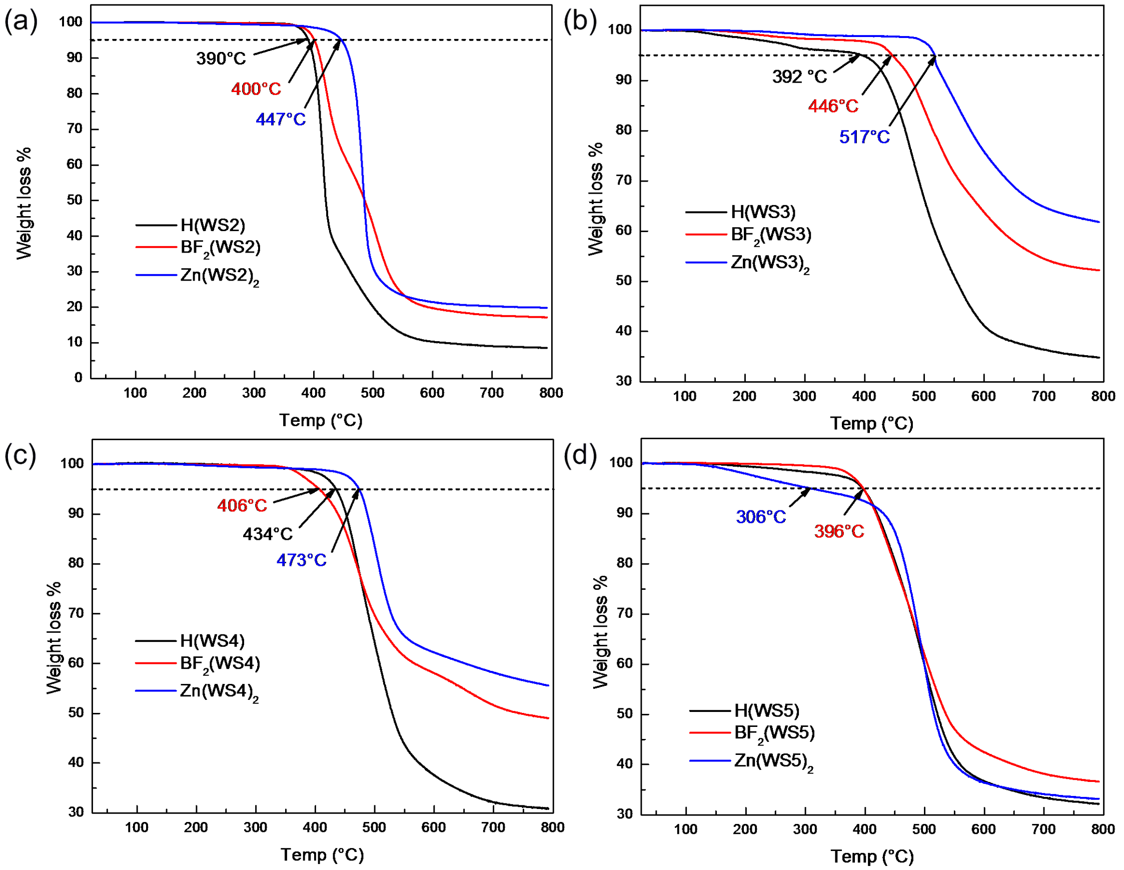

Figure S13. TGA graphs of (a) H(WS2), BF$_2$(WS2), and Zn(WS2)$_2$, (b) H(WS3), BF$_2$(WS3), and Zn(WS3)$_2$, (c) H(WS4), BF$_2$(WS4), and Zn(WS4)$_2$, and (d) H(WS5), BF$_2$(WS5), and Zn(WS5)$_2$.

Table S1. Decomposition temperature (°C) at 5% weight loss.

	(ADP)	(WS1)	(WS2)	(WS3)	(WS4)	(WS5)
H	356	280	390	392	434	396
BF_2^+	372	375	400	446	406	396
Zn(II)	461	304	447	517	473	306

Cyclic Voltammetry

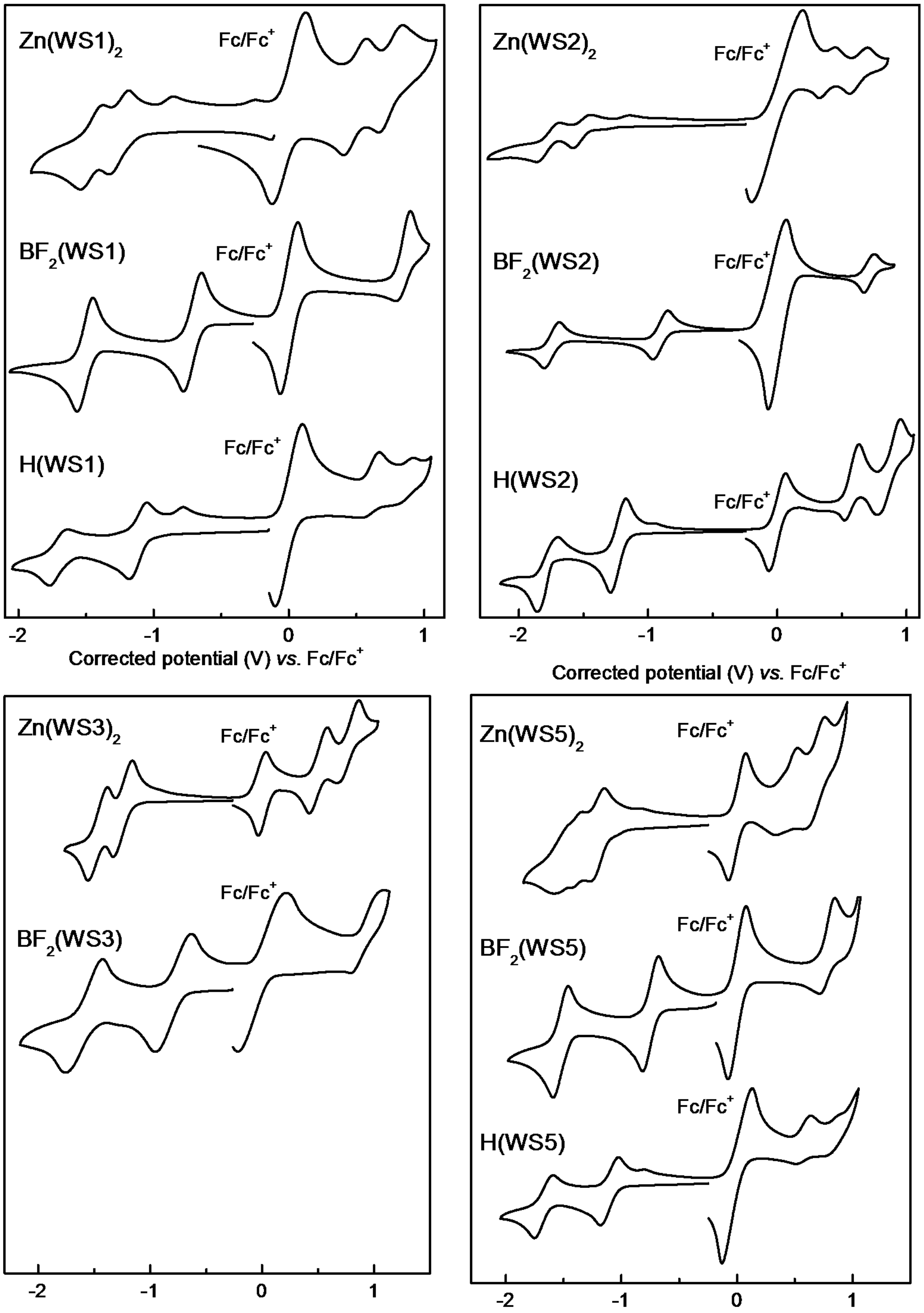

Figure S14. Cyclic voltammetry plots of representative H^+, BF_2^+ and Zn^{+2} chelates of WS1, WS2, WS3 and WS5 ligands in 0.1 M TBAPF dichloromethane solution and Fc/Fc$^+$ as internal standard.

Table S2. Onsets for the oxidation and reduction.

	Oxidation onset (V vs Fc/Fc+)	Reduction onset (V vs Fc/Fc+)
H(ADP)	0.50	-1.11
BF_2(ADP)	0.80	-0.73
Zn$(ADP)_2$	0.34	-1.34
H(WS1)	0.55	-1.03
BF_2(WS1)	0.78	-0.63
Zn$(WS1)_2$	0.45	-1.13
H(WS2)	0.50	-1.15
BF_2(WS2)	0.63	-0.83
Zn$(WS2)_2$	0.38	-1.46
H(WS3)	-	-
BF_2(WS3)	0.86	-0.70
Zn$(WS3)_2$	0.42	-1.16
H(WS4)	0.45	-1.09
BF_2(WS4)	0.71	-0.75
Zn$(WS4)_2$	0.38	-1.21
H(WS5)	0.51	-1.02
BF_2(WS5)	0.71	-0.67
Zn$(WS5)_2$	0.38	-1.09

Optical Properties

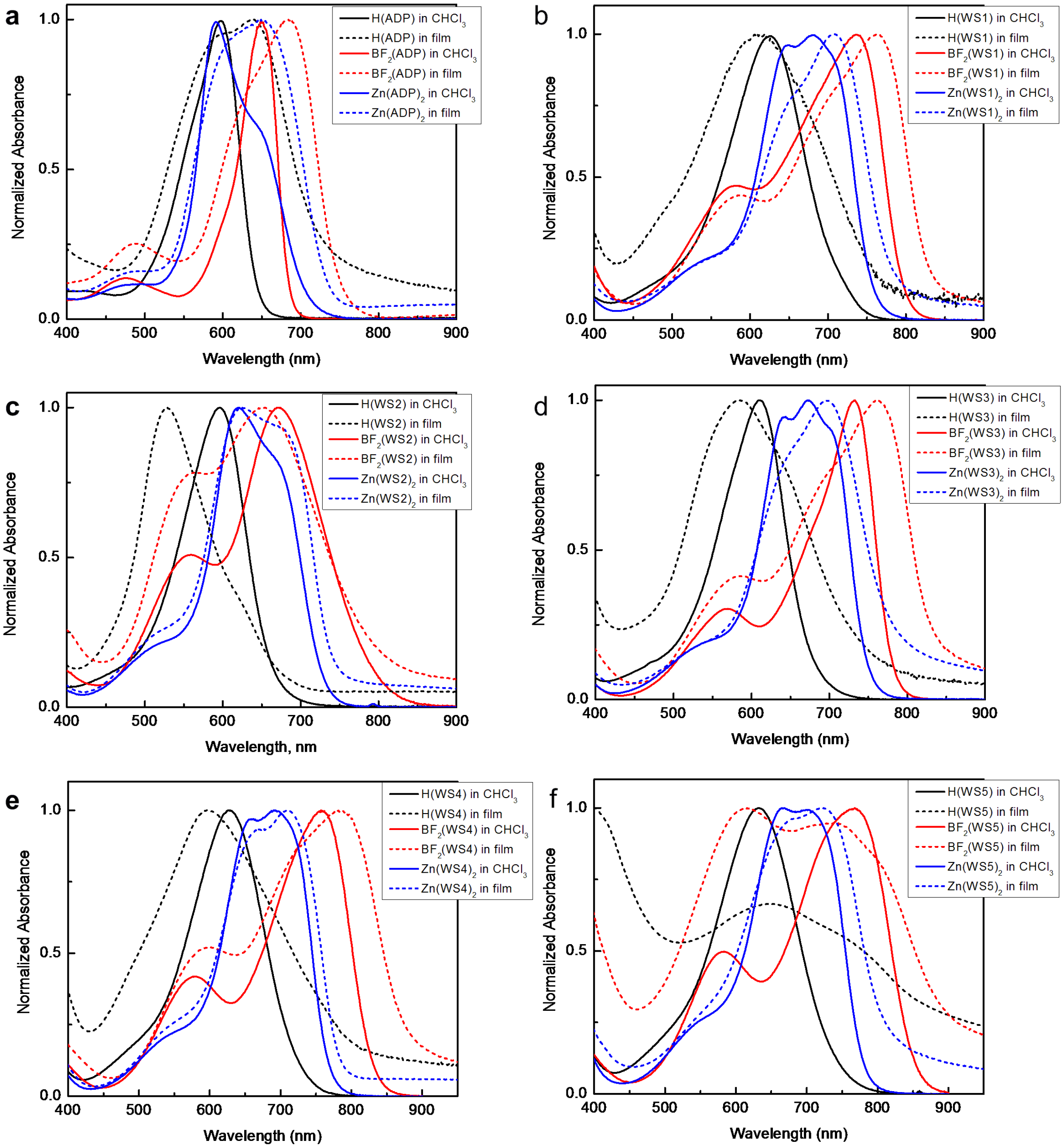

Figure S15. Absorption spectra of ADP-based molecules in chloroform and in films.

The spectra were normalized to the low energy absorption maximum for easier comparison.

Table S3. Additional optical properties of ADP-based molecules and their blends with P3HT.

Acceptor	Shift from solution to film of acceptor		P3HT:acceptor blend film
	$\lambda_{max}^{visible}$, nm	$\lambda_{onset}^{visible}$, nm	λ_{onset}, nm
H(ADP)	+44	+95	657
BF_2(ADP)	+62	+122	753
Zn$(ADP)_2$	+59	+22	740
H(WS1)	-13	+50	667
BF_2(WS1)	+22	+37	830
Zn$(WS1)_2$	+24	+16	790
H(WS2)	-66	+16	650
BF_2(WS2)	-17	-5	730
Zn$(WS2)_2$	+2	+8	745
H(WS3)	-25	+99	660
BF_2(WS3)	+31	+63	812
Zn$(WS3)_2$	+22	+28	786
H(WS4)	-32	+95	675
BF_2(WS4)	+23	+50	885
Zn$(WS4)_2$	+16	+5	790
H(WS5)	+12	+134	665
BF_2(WS5)	-18	+40	895
Zn$(WS5)_2$	+57	+35	800

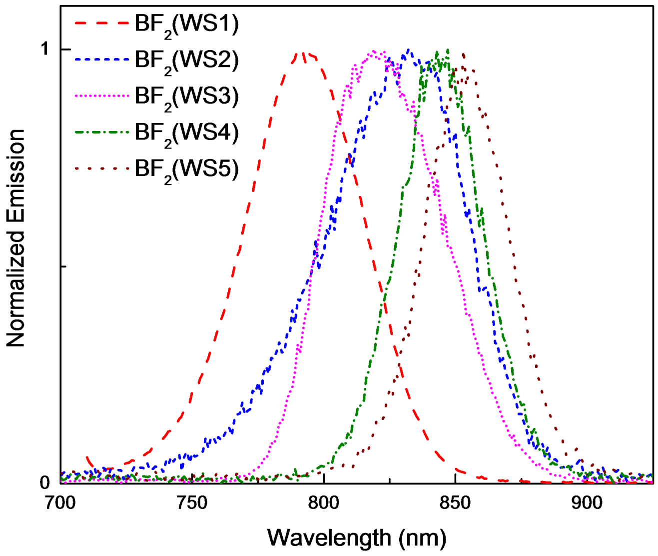

Figure S16. Emission spectra of ADP-based BF_2^+ chelates in chloroform.

Table S4. Emission properties of ADP-based BF_2^+ chelates in chloroform. Excitation wavelength is 600 nm.

Compound	Emission λ_{max}, nm
BF_2(WS1)	794
BF_2(WS2)	830
BF_2(WS3)	820
BF_2(WS4)	843
BF_2(WS5)	853

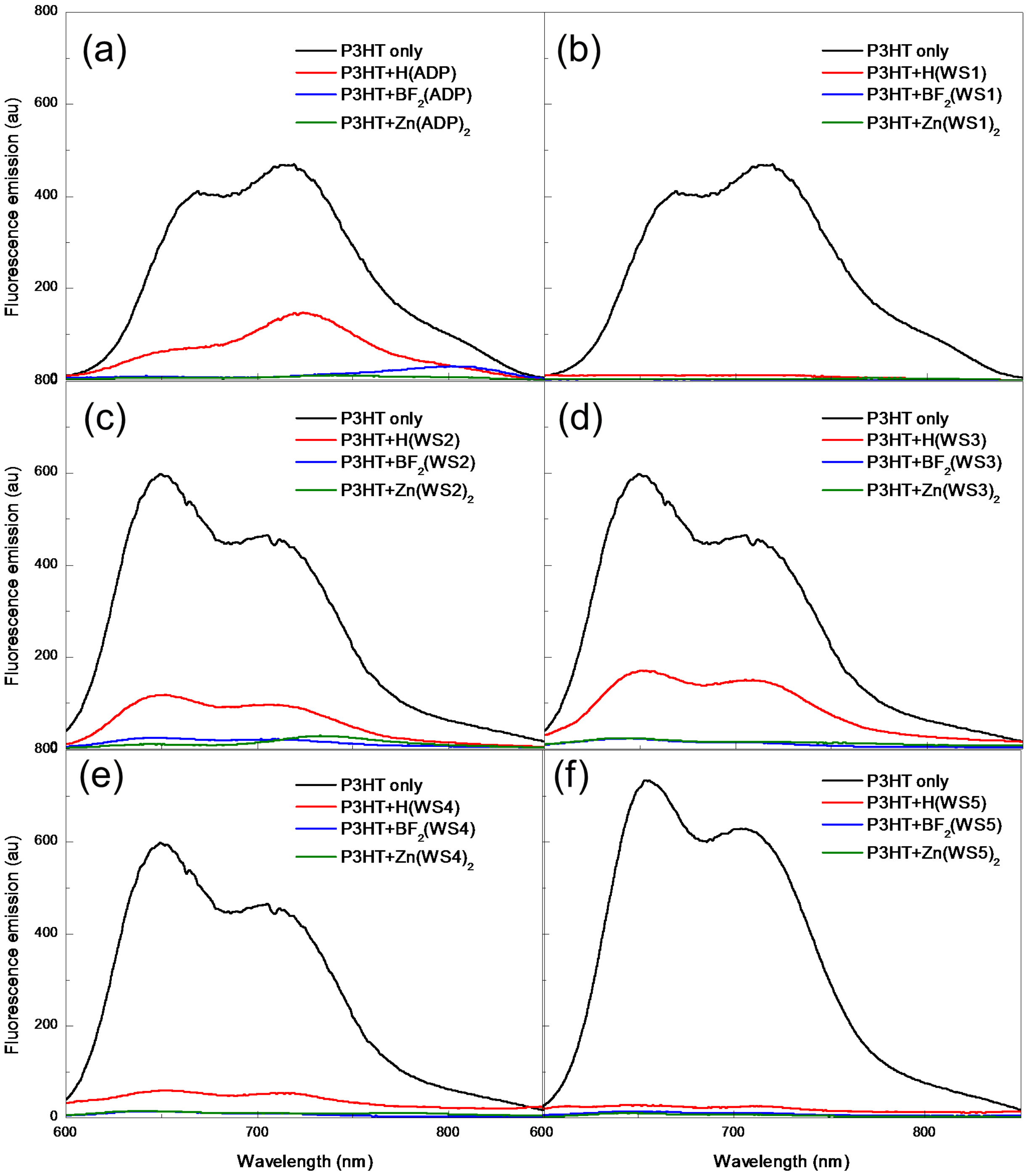

Figure S17. P3HT Fluorescence quenching with new ADP-based molecules in films.

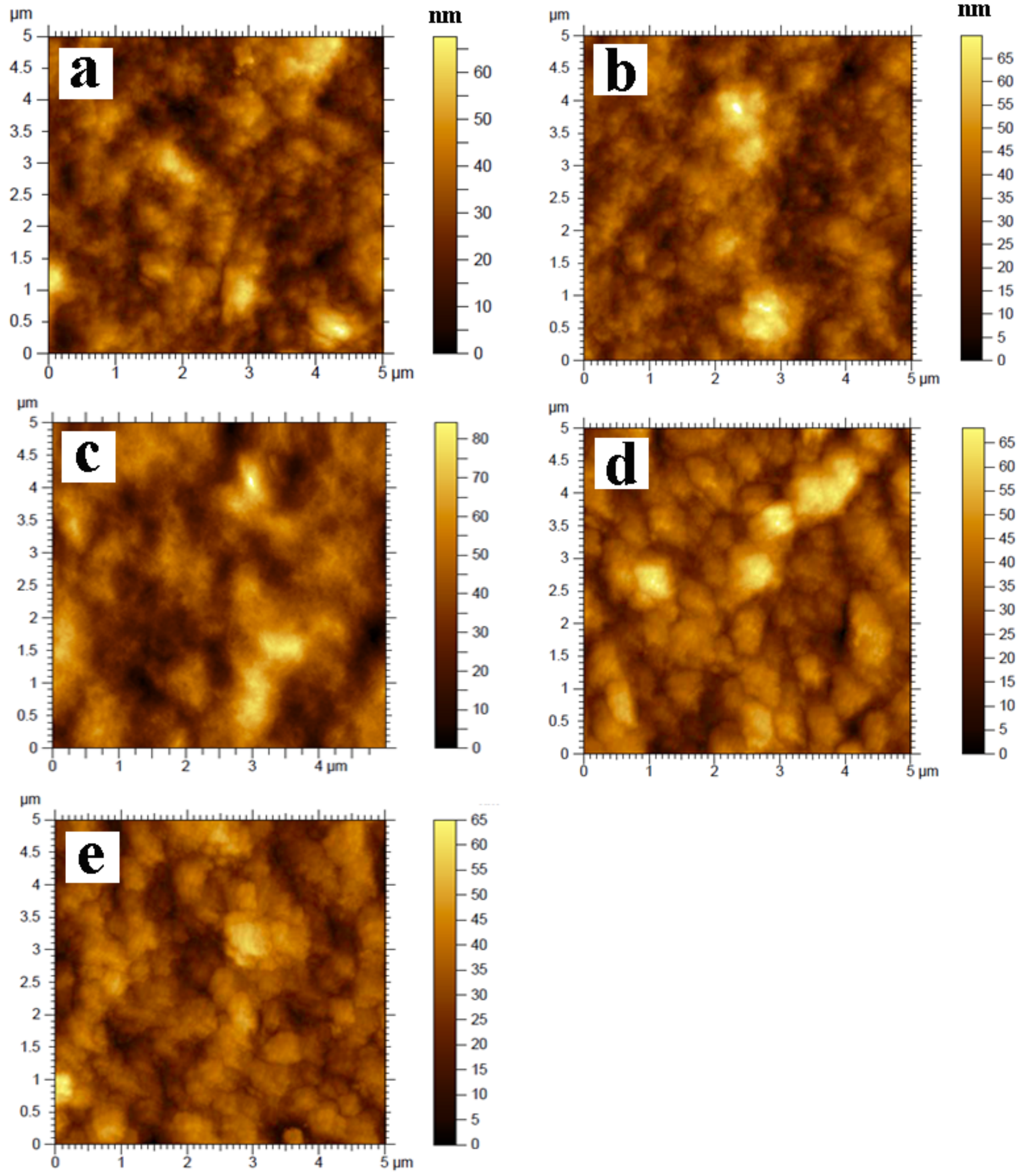

Figure S18. Tapping-mode AFM height images (a-e) for P3HT:acceptor blends taken directly from the active layers of the best cells reported in Table 3. The acceptor was: (a) Zn(WS1)$_2$; (b) Zn(WS2)$_2$; (c) Zn(WS3)$_2$; (d) Zn(WS4)$_2$; (e) Zn(WS5)$_2$. All images are 5 µm × 5 µm.

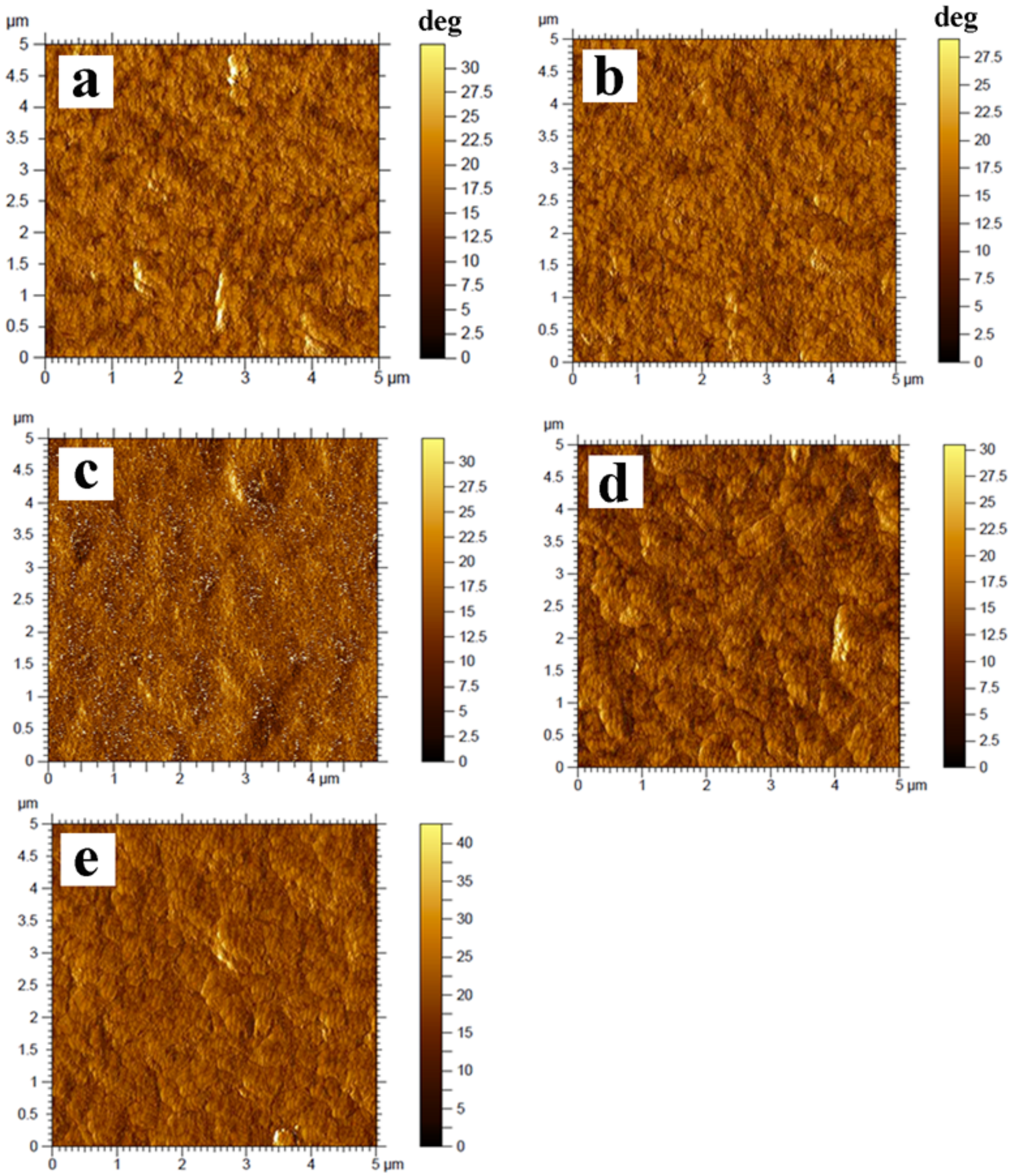

Figure S19. Tapping-mode AFM phase images (a-e) for P3HT:acceptor blends taken directly from the active layers of the best cells reported in Table 3. The acceptor was: (a) Zn(WS1)$_2$; (b) Zn(WS2)$_2$; (c) Zn(WS3)$_2$; (d) Zn(WS4)$_2$; (e) Zn(WS5)$_2$. All images are 5 µm × 5 µm.

Table S5. Screening of organic solar cells using free ligands and BF2 chelates as acceptors.

	Weight ratio	V_{oc} (V)	J_{sc}	FF	PCE (%)
P3HT:ADP	1:1	0.90	0.034	27	0.0084
P3HT:ADP	1:2	0.83	0.043	25	0.0089
P3HT:WS1	1:2	0	0	0	0
P3HT:WS2	1:2	0	0	0	0
P3HT:WS3	1:2	0	0	0	0
P3HT:WS4	1:2	0	0	0	0
P3HT:WS5	1:2	0	0	0	0
P3HT:BF_2(WS1)	1:2	0.036	2.38	0.22	0.19
P3HT:BF_2(WS2)	1:2	0.11	0.83	0.27	0.024
P3HT:BF_2(WS3)	1:2	0.02	1.87	0.22	0.0067
P3HT:BF_2(WS4)	1:2	0.02	0.65	0.21	0.0027
P3HT:BF_2(WS5)	1:2	0.02	0.68	0.25	0.0033

* Total concentration: 20 mg/mL, solvent: DCB, spin-coated 100 rpm for 40 s then 2000 rpm for 2 s, annealed at 120C for 15 min prior to top electrode deposition.

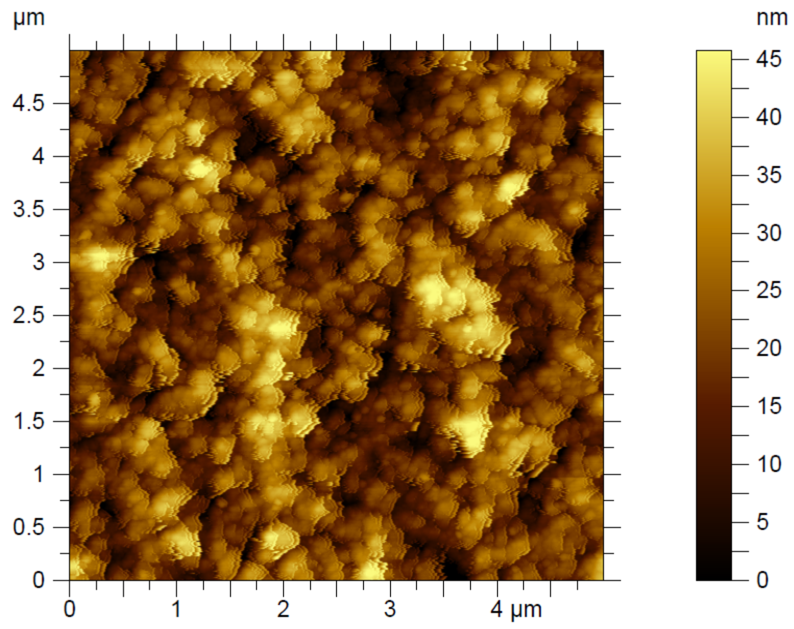

Figure S20. Tapping-mode AFM phase images of P3HT:BF$_2$(ADP) blend (1:1 weight ratio).

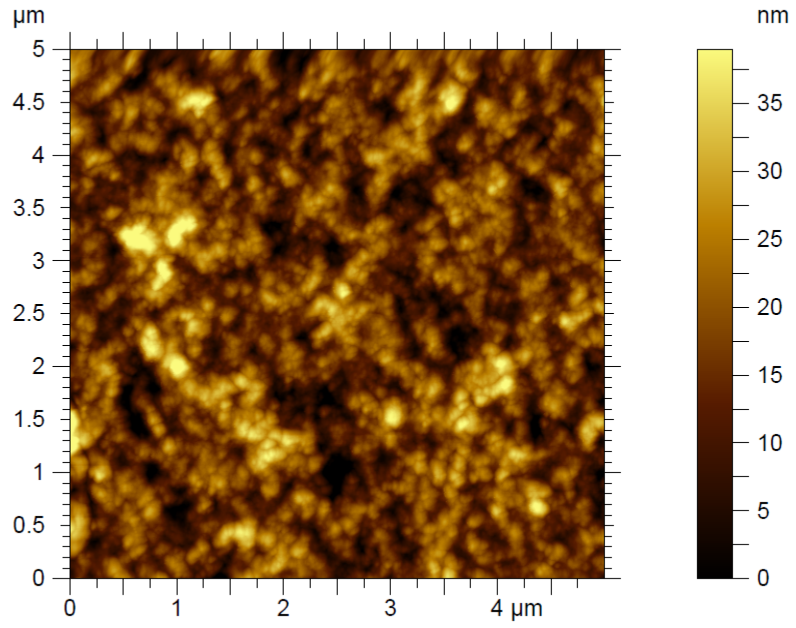

Figure S21. Tapping-mode AFM phase images of P3HT:BF$_2$(WS1) blend (1:1 weight ratio).

References

[S1] Xia, C.; Fan, X.; Locklin, J.; Advincula, R. C. *Org. Lett.* **2002**, *4*, 2067.